Electronic Supplementary Material (ESI) for Journal of Materials Chemistry C.
This journal is © The Royal Society of Chemistry 2022

Electronic Supplement Material (ESI) for Journal of Materials Chemistry C

Multi-functional hybrid perovskites with triple-channel switches and optical properties

Meng-Meng Lun, Fo-Ling Zhou, Da-Wei Fu *, Qiong Ye*

Ordered Matter Science Research Center, Jiangsu Key Laboratory for Science and Applications of Molecular Ferroelectrics, Southeast University, Nanjing, 211189, People's Republic of China.
*Corresponding author (E-mail: dawei@seu.edu.cn; yeqiong@seu.edu.cn)

Experimental Measurement Methods

Single-crystal X-ray Diffraction (SXRD). The crystallographic structures of compounds were identified using a Rigaku single-crystal X-ray diffractometer with Mo-Kα radiation (*λ*= 0.71073 Å). The structures of samples were determined by direct methods and refined by the full matrix method through the SHELXTL software package. All non-hydrogen atoms were refined anisotropically, and all hydrogen atoms which were generated geometrically possessed isotropic displacement parameters. The crystallographic information and structure refinement of compounds are summarized in Table S1. The selected bond lengths and angles of compounds are also displayed in Table S2 and S3. Moreover, the crystallographic structures of compounds have been deposited at the Cambridge Crystallographic Data Center (CCDC) (deposition numbers: 2094204, 2094248, 2096017, 2072355, 2067453, 2094448) and can be obtained free of charge from the CCDC *via* www.ccdc.cam.ac.uk/getstructures.

Powder X-ray Diffraction (PXRD). The powder X-ray diffraction patterns of microcrystalline compounds were characterized by a Rigaku D-MAX diffraction system under Cu-kα radiation in the 2θ range from 5° to 50° with a step size of 0.02° at 298 K. Simulated powder patterns of samples were calculated by Mercury software package using the crystallographic information file from the single-crystal X-ray experiment.

Infrared (IR) Spectrometry. The IR spectra of compounds were performed at room temperature by a Shimadzu IR-60 spectrometer in the range from 4000 to 400 cm^{-1}.

Dielectric. For dielectric characterization, these crystals were ground to become powders, then pressed into a plate with 0.45 mm thickness. Both plate surfaces were coated with silver paste and dried in an oven at 333 K for 5 h. The plate was then used as an electrode to record the curve of temperature-dependent dielectric permittivity ε through a Tonghui TH2828A Precision LCR meter with an AC voltage of 1 V. The complex dielectric permittivity ε ($\varepsilon = \varepsilon^{'} - \varepsilon^{''}$), where ε' is the real part, and ε'' is the imaginary part.

Differential Scanning Calorimetry (DSC). DSC curves of compounds were recorded by a NETZSCH-214 instrument, and microcrystalline compounds were heated and cooled in an aluminum crucible with the rate of 20 K min^{-1} in the temperature range of 265-430 K.

Thermogravimetry (TG). TG curves of compounds were characterized by a NETZSCH STA 449F5 instrument, and microcrystalline compounds were heated and cooled in an aluminum crucible with the rate of 10 K min^{-1} in the temperature range of 293-1073 K.

Second Harmonic Generation (SHG). SHG signals of samples were recorded by an Edinburgh FLS920 instrument equipped with an Nd:YAG laser (λ = 1064 nm, Vibrant 355 II, OPOTEK), which can emit unexpanded laser beam with low divergence.

UV-visible (UV-vis) Spectrophotometry. UV-vis absorption spectra of samples were performed by a Shimadzu 2550PC spectrophotometry with $BaSO_4$ employed as a reference sample at room temperature.

Fluorescence Spectrofluorometer. The emission and excitation spectra of samples were measured using an Edinburgh FLS1000 fluorescence spectrophotometer equipped with a xenon lamp as the excitation source, and time-resolved spectra were recorded through the Edinburgh spectrophotometer equipped with a nanosecond pulsed hydrogen lamp. The photoluminescence quantum efficiency of compounds was characterized using an integrating sphere in the spectrofluorometer. The CIE chromaticity coordinates were calculated using the CIE software package based on the emission spectrum data.

Hirshfeld Surfaces Analysis. Hirshfeld surfaces and the associated 2D fingerprint plots were calculated by the CrystalExplorer software package by inputting the crystallographic structure files of compounds generated by SXRD. Hirshfeld surfaces of three compounds were obtained using a high surface resolution, which can provide the information about intermolecular interactions in the crystal. The 2D fingerprint plot is a combination of d_e and d_i that provides the summary of intermolecular contacts in the crystal and are as a useful complement to the Hirshfeld surfaces, where d_i is the distance to the nearest atom center interior to the surface, and d_e exterior to the surface. The normalized contact distance d_{norm} is based on d_e, d_i and the van der Waals (vdW) radii of the two atoms external (r_e^{vdW}) and internal (r_i^{vdW}) to the surface:

$$d_{norm} = \frac{d_i - r^{vdW}}{r_i^{vdW}} + \frac{d_e - r}{r_e^{vdW}}$$

d_{norm} surface is used for the identification of close intermolecular interactions. The value d_{norm} is negative or positive when intermolecular contacts are shorter or longer than r^{vdW}, respectively. Hirshfeld surface with d_{norm} values display a red-blue-white color scheme: where red regions correspond to closer contacts and negative d_{norm} value; the blue regions correspond to longer contacts and positive d_{norm} value; and the white regions correspond to the distance of contacts is exactly the van der Waals separation and with a d_{norm} value of zero.

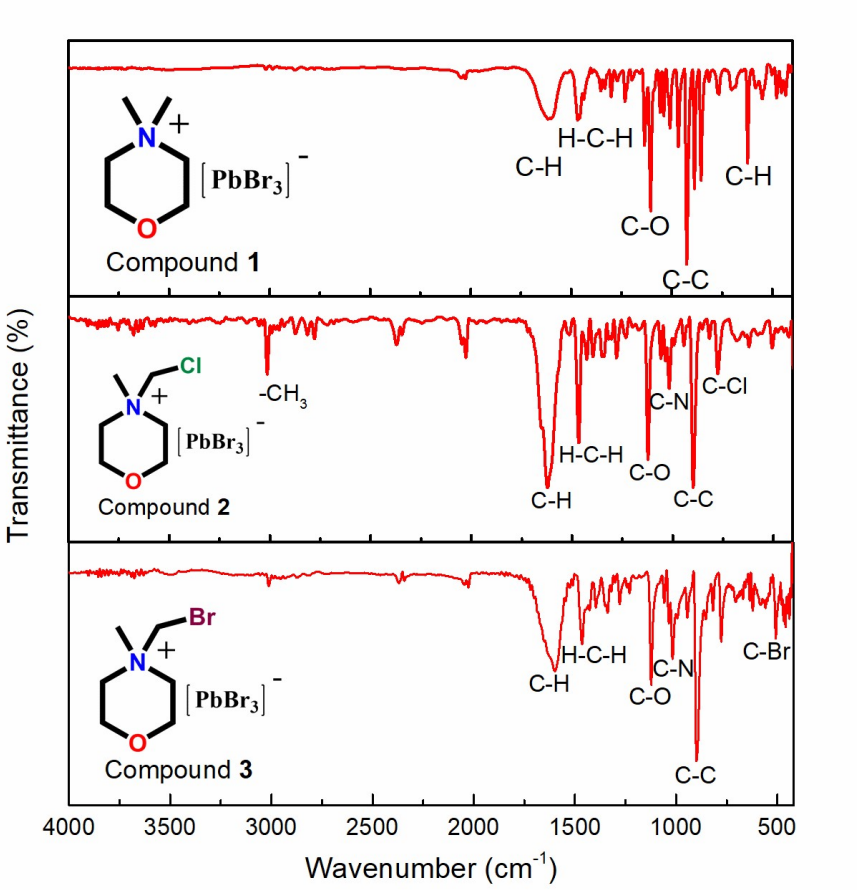

Figure S1. IR spectra of compounds measured at room temperature. The peaks at approximately 775 and 507 cm^{-1} are assigned to the characteristic absorption of C-Cl bond within compound **2** and C-Br bond within compound **3**, respectively.

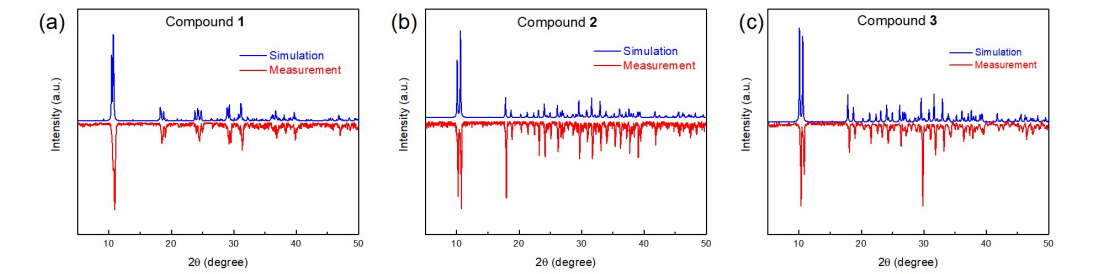

Figure S2. The measured and simulated PXRD patterns of compounds are well matched, verifying the phase purity of the compounds.

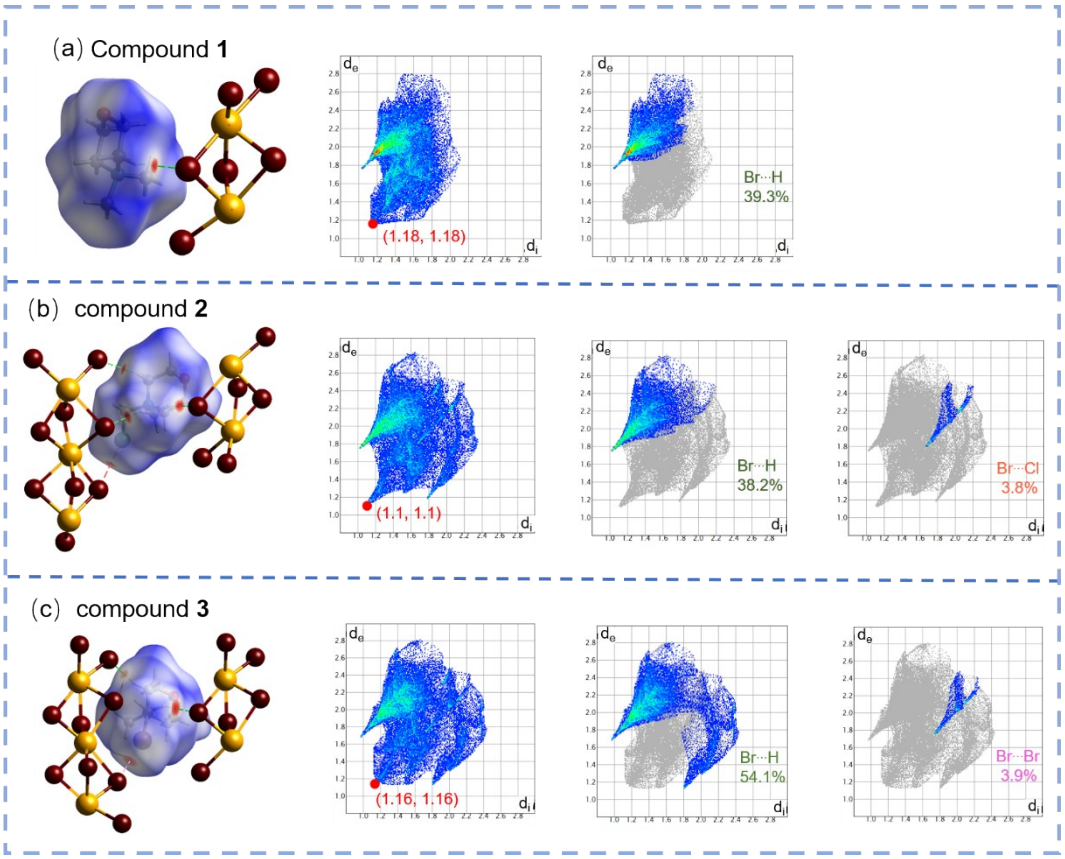

Figure S3 Hirshfeld d_{norm} surfaces and 2D fingerprint plots of compound **1**, **2** and **3**. The green, red and purple dot lines denote C-H…Br-Pb, C-Cl…Br-Pb and C-Br…Br-Pb weak interactions, respectively.

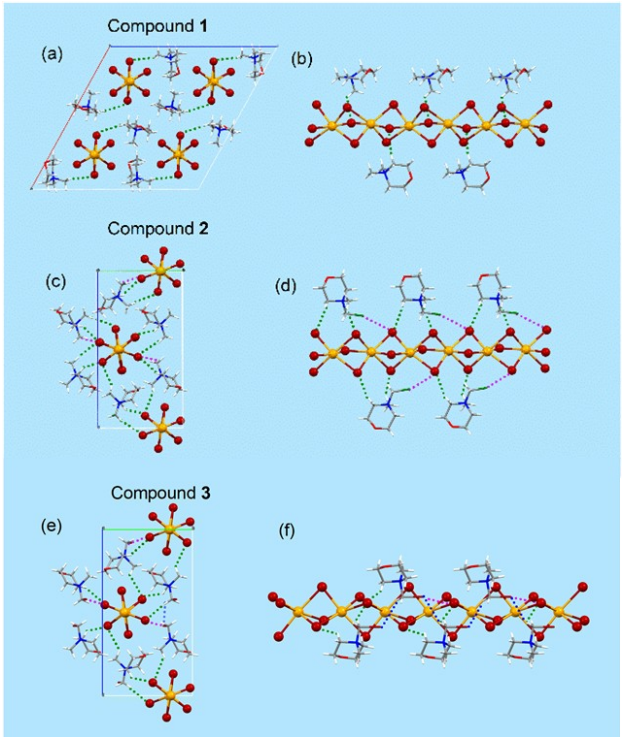

Figure S4. The weak interactions of **1**, **2** and **3** between organic cations and inorganic $[PbBr_6]^-$ infinite chains. The green and purple dashed lines denote the C-H···Br-Pb and C-X···Br-Pb (X=Cl, Br) weak interactions, respectively. The blue dashed lines denote the weak interactions among the organic cations in compound **3**.

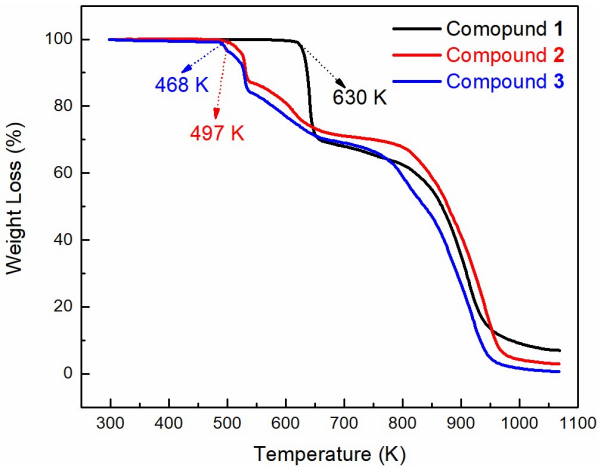

Figure S5. TG curves of compounds in the temperature range from 293 to 1073 K.

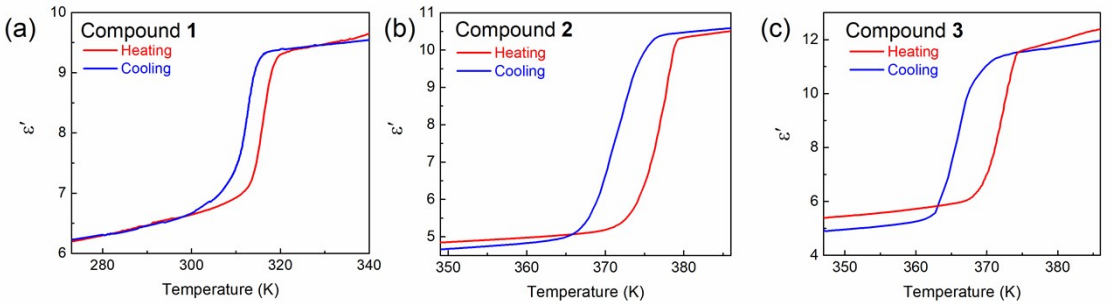

Figure S6. Temperature-dependent of ε' for **1** (a), **2** (b), and **3** (c) at 1 MHz.

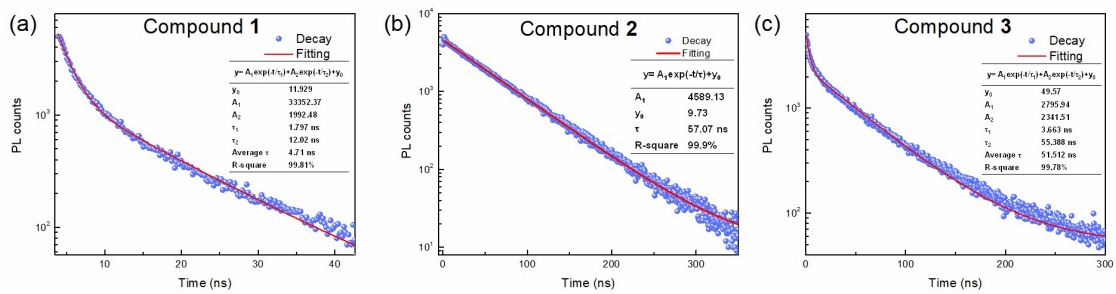

Figure S7. Decay curves and calculated luminescence lifetimes of **1** (a), **2** (b), and **3** (c) at room temperature.

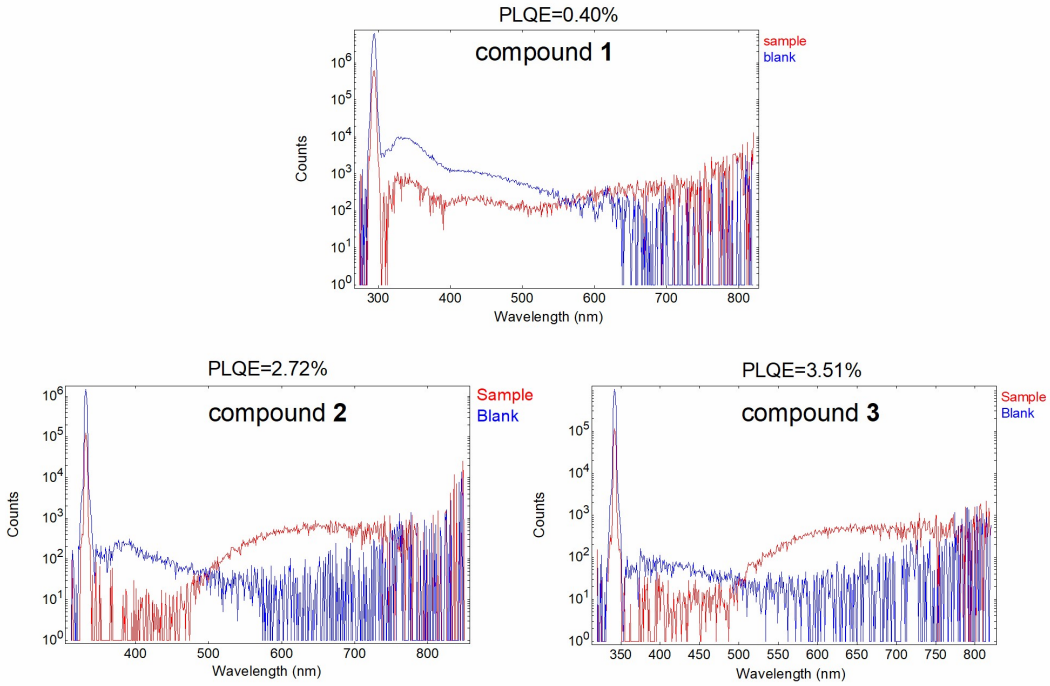

Figure S8. The photoluminescence quantum efficiency of compounds at room temperature.

Table S1. Crystal data and structure refinement for compounds.

Compound	Compound **1**		Compound **2**		Compound **3**	
Empirical formula	$C_6H_{14}NOPbBr_3$	$C_6H_{14}NOPbBr_3$	$C_6H_{13}NOClPbBr_3$	$C_6H_{13}NOClPbBr_3$	$C_6H_{13}NOClPbBr_4$	$C_6H_{13}NOClPbBr_4$
Formula weight	563.08	563.08	597.54	597.54	642	642
Crystal system	Monoclinic	Hexagonal	Orthorhombic	Trigonal	Orthorhombic	Trigonal
Space group	$P2_1/c$ (No.14)	$P6_3/mmc$ (No. 194)	$P2_12_12_1$ (No. 19)	$P\bar{3}c1$ (No. 165)	$P2_12_12_1$ (No. 19)	$P\bar{3}c1$ (No. 165)
Temperature	293 K	328 K	298 K	383 K	293 K	383 K
a (Å)	18.8860(8)	9.8400(7)	8.0374 (3)	17.4023 (3)	8.0355(2)	17.425(2)
b (Å)	7.9709(2)	9.8400(7)	9.4801 (4)	17.4023 (3)	9.4769(2)	17.425(2)
c (Å)	19.3167(9)	7.8271(5)	17.5303 (8)	7.9318 (2)	17.5267(4)	7.9527(16)
α	90°	90°	90°	90°	90°	90°
β	118.766(6) °	90°	90°	90°	90°	90°
γ	90°	120°	90°	120°	90°	120°
V (Å^3)	2549.0(2)	656.33(10)	1335.73 (10)	2080.25 (7)	1334.59(5)	2091.1(7)
Z	4	2	4	2	4	2
Radiation	Mo-K_α	Mo-K_α	Mo-K_α	Mo-K_α	Mo-K_α	Mo-K_α
CCDC number	2094204	2094248	2096017	2072355	2067453	2094448
Calculated density (g/cm^3)	2.935	3.112	2.971	3.735	3.195	3.995
Melting point	513 K	513 K	468 K	468 K	450 K	450 K
Absorption coefficient (mm^{-1})	22.61	21.97	21.773	27.96	24.58	31.38
F (000)	2016	542	1072.0	2040.0	1144	2184

Data collection range	2.1-29.7°	2.4-23.0°	2.32-30.498°	2.34-24.97°	2.32-30.44°	2.3-22.783°
R (int)	0.059	0.030	0.099	0.064	0.085	0.156
Completeness to θ	0.999	0.901	1.75/1.00	99.9%	1.75/1.00	99.9%
Data, restraints, parameters	4494, 170, 147	364, 42, 23	4086, 81, 119	1224, 17, 83	4090, 1, 119	951, 66, 103
Goodness-of-fit on F^2	1.04	1.12	1.129	1.176	1.068	2.070
R_1, $wR_2[I > 2\sigma(I)]$	0.084, 0.2096	0.058, 0.1896	0.0272, 0.0544	0.1587, 0.2931	0.0502, 0.1554	0.1720, 0.4790
$\Delta\rho_{max}$, $\Delta\rho_{min}$ (e $Å^{-3}$)	4.38, -4.47	0.83, -1.47	0.78, -4.52	4.31, -6.45	2.09, -4.35	5.76, -3.05

Table S2. The selected bond lengths and angles for compounds at room time

Bond lengths (Å) and bond angles (°)					
Compound **1** at 293 K		Compound **2** at 298 K		Compound **3** at 293 K	
Br1-Pb1	3.0089(9)	Pb1- Br1	3.2285(8)	Pb1-Br2	2.8756(6)
Br1-Pb2^{i}	3.1004(9)	Pb1- Br1^{1}	2.9305(8)	Pb1-Br2^{1}	3.2177(6)
Br2-Pb1	3.2129(10)	Pb1- Br2^{2}	2.8729(8)	Pb1-Br3^{2}	3.2319(6)
Br2-Pb2^{i}	2.8727(11)	Pb1- Br2	3.2197(8)	Pb1-Br3	2.8735(5)
Br3-Pb1	2.9033(8)	Pb1- Br3^{2}	3.2322(7)	Pb1-Br4^{2}	3.2285(6)
Br4-Pb1	2.9171(12)	Pb1- Br3	2.8742(7)	Pb1-Br4	2.9296(6)
Br5-Pb1	3.0240(7)	Br1- Pb1^{2}	2.9304(8)	Br4-Pb1^{1}	3.2285(6)
Br5-Pb2	2.9846(7)	Br2- Pb1^{1}	2.8729(8)	Br2-Pb1^{2}	3.2177(6)
Br6-Pb2	2.8812(9)	Br3- Pb1^{1}	3.2322(7)	Br3-Pb1^{1}	3.2319(6)
Pb1-Br1-Pb2^{i}	81.65(2)	Br1^{1}-Pb1-Br1	174.06(2)	Br2-Pb1-Br2^{1}	168.997(18)
Pb2^{i}-Br2-Pb1	81.85(3)	Br1^{1}-Pb1-Br2	80.87(2)	Br2^{1}-Pb1-Br3^{2}	107.658(15)
Pb2-Br5-Pb1	83.177(17)	Br1^{1}-Pb1-Br3^{2}	101.68(2)	Br2-Pb1-Br3^{2}	82.343(16)
Br1-Pb1-Br2	82.92(3)	Br1-Pb1-Br3^{2}	76.080(19)	Br2^{1}-Pb1-Br4^{2}	104.971(15)
Br3-Pb1-Br1	88.40(3)	Br2-Pb1-Br1	105.03(2)	Br2-Pb1-Br4^{2}	81.563(16)
Br3-Pb1-Br2	77.56(2)	Br2^{2}-Pb1-Br1^{1}	92.70(2)	Br2-Pb1-Br4	92.705(17)
Br3-Pb1-Br4	88.00(3)	Br2^{2}-Pb1-Br1	81.58(2)	Br3-Pb1-Br2	88.062(17)
Br3-Pb1-Br5	92.39(2)	Br2^{2}-Pb1-Br2	168.90(2)	Br3-Pb1-Br2^{1}	82.627(15)

Br4-Pb1-Br1	91.86(4)	Br2^{2}-Pb1-Br3^{2}	82.35(2)	Br3-Pb1-Br3^{2}	167.558(17)
Br4-Pb1-Br2	164.74(3)	Br2^{2}-Pb1-Br^{3}	88.07(2)	Br3-Pb1-Br4	86.580(17)
Br4-Pb1-Br5	86.28(2)	Br2-Pb1-Br3^{2}	107.73(2)	Br3-Pb1-Br4^{2}	94.783(16)
Br5-Pb1-Br2	99.09(2)	Br3-Pb1-Br1	94.76(2)	Br4-Pb1-Br2^{1}	80.941(16)
Br2^{ii}-Pb2-Br1^{ii}	87.20(3)	Br3-Pb1-Br1^{1}	86.60(2)	Br4-Pb1-Br3^{2}	101.708(16)
Br2^{ii}-Pb2-Br5	87.56(2)	Br3-Pb1-Br2	82.55(2)	Br4^{2}-Pb1-Br3^{2}	76.044(15)
Br2^{ii}-Pb2-Br6	93.25(3)	Br3-Pb1-Br3^{2}	167.57(2)	Br4-Pb1-Br4^{2}	174.048(15)
Br5-Pb2-Br1^{ii}	172.39(4)	Pb1^{2}-Br1-Pb1	81.392(18)	Pb1-Br2-Pb1^{2}	82.388(14)
Br6-Pb2-Br1^{ii}	90.04(3)	Pb1^{1}-Br2-Pb1	82.419(19)	Pb1-Br3-Pb1^{1}	82.167(13)
Br6-Pb2-Br5	84.77(2)	Pb1-Br3-Pb1^{1}	82.176(17)	Pb1-Br4-Pb1^{1}	81.382(13)

Symmetry codes: (i) *x*, *y*−1, *z*; (ii) *x*, *y*+1, *z*. (1) -1/2+X,1/2-Y,1-Z; (2) 1/2+X,1/2-Y,1-Z

Table S3. The selected bond lengths and angles for compounds at high temperature.

Bond lengths (Å) and bond angles (°)					
Compound **1** at 328 K		Compound **2** at 383 K		Compound **3** at 383 K	
Pb1-Br1^{i}	3.0405(10)	Pb1-Br1^{1}	2.958(2)	Pb1-Br1	2.9504(17)
Pb1-Br1^{ii}	3.0405(10)	Pb1-Br1^{2}	3.089(2)	Pb1-Br1^{1}	3.1168(18)
Pb1-Br1^{iii}	3.0405(10)	Pb1-Br1^{3}	3.089(2)	Pb1-Br1^{2}	3.1168(18)
Pb1-Br1^{iv}	3.0405(10)	Pb1-Br1	2.958(2)	Pb1-Br1^{3}	2.9505(17)
Pb1-Br1^{v}	3.0405(10)	Pb1-Br1^{4}	2.958(2)	Pb1-Br1^{4}	2.9505(17)
Pb1-Br1	3.0405(10)	Pb1-Br1^{5}	3.089(2)	Pb1-Br1^{5}	3.1168(18)
Br1-Pb1^{vi}	3.0405(10)	Br1-Pb1^{6}	3.089(2)	Br1-Pb1^{6}	3.1167(18)
Br1^{i}-Pb1-Br1^{iii}	83.03(2)	Br2-Pb2^{8}	2.974(4)	Br2-Pb2	2.3859(14)
Br1^{ii}-Pb1-Br1^{iii}	96.97(2)	Br2-Pb2^{7}	3.103(4)	Br2-Pb2^{7}	3.037(2)
Br1^{i}-Pb1-Br1^{iv}	96.97(2)	Br2-Pb2	2.449(4)	Br2-Pb2^{8}	2.919(2)
Br1^{ii}-Pb1-Br1^{iv}	83.03(2)	Pb2-Br2^{9}	2.449(4)	Pb2-Br2^{10}	3.037(2)
Br1^{iii}-Pb1-Br1^{iv}	96.97(2)	Pb2-Br2^{10}	3.103(4)	Pb2-Br2^{11}	3.037(2)
Br1^{i}-Pb1-Br1^{v}	83.03(2)	Pb2-Br2^{7}	3.103(4)	Pb2-Br2^{12}	2.3858(14)
Br1^{ii}-Pb1-Br1^{v}	96.97(2)	Pb2-Br2^{11}	2.974(4)	Pb2-Br2^{9}	2.919(2)

Br1^{iii}-Pb1-Br1^{v}	83.03(2)	Pb2-Br2^{12}	3.103(4)	Pb2-Br2^{13}	2.3860(14)
Br1^{i}-Pb1-Br1	96.97(2)	Pb2-Br2^{13}	2.974(4)	Pb2-Br2^{7}	3.037(2)
Br1^{ii}-Pb1-Br1	83.03(2)	Pb2-Br2^{8}	2.974(4)	Pb2-Br2^{14}	2.919(2)
Br1^{iv}-Pb1-Br1	83.03(2)	Pb2-Br2^{14}	2.449(4)	Pb2-Br2^{8}	2.919(2)
Br1^{v}-Pb1-Br1	96.97(2)	Br1^{1}-Pb1-Br1	83.80(7)	Br1-Pb1-Br1^{1}	84.44(6)
Pb1^{vi}-Br1-Pb1	80.12(3)	Br1^{2}-Pb1-Br1^{3}	98.29(10)	Br1^{2}-Pb1-Br1^{3}	98.05(5)
		Br1^{4}-Pb1-Br1^{5}	79.51(7)	Br1^{4}-Pb1-Br1^{5}	79.00(5)
		Br1^{1}-Pb1-Br1^{2}	83.80(7)	Br1-Pb1-Br1^{2}	84.44(6)
		Br1-Pb1-Br1^{5}	98.29(10)	Br1^{1}-Pb1-Br1^{5}	176.37(6)
		Br1-Pb1-Br1^{2}	83.80(7)	Br1^{1}-Pb1-Br1^{2}	84.44(6)
		Br1-Pb1-Br1^{3}	177.14(8)	Br1^{1}-Pb1-Br1^{3}	98.41(6)
		Br11-Pb1-Br1^{4}	98.29(10)	Br1-Pb1-Br1^{4}	98.41(6)
		Br1^{4}-Pb1-Br1^{3}	79.51(7)	Br1^{4}-Pb1-Br1^{3}	79.00(5)
		Br1-Pb1-Br1^{4}	98.33(10)	Br1^{1}-Pb1-Br1^{4}	98.05(5)
		Br1^{2}-Pb1-Br1^{5}	98.33(10)	Br1^{2}-Pb1-Br1^{5}	98.41(6)
		Br1^{2}-Pb1-Br1^{4}	177.14(8)	Br1^{2}-Pb1-Br1^{4}	176.37(6)
		Br1^{3}-Pb1-Br1^{5}	79.51(7)	Br1^{3}-Pb1-Br1^{5}	79.00(5)
		Br1^{1}-Pb1-Br1^{3}	98.33(10)	Br1-Pb1-Br1^{3}	176.37(6)
		Br1^{1}-Pb1-Br1^{5}	177.14(8)	Br1-Pb1-Br1^{5}	98.06(5)
		Pb1-Br1-Pb1^{6}	81.94(5)	Pb1-Br1-Pb1^{6}	81.85(3)

Symmetry codes: (i) *x*−*y*, *x*−1, −*z*+1; (ii) −*x*+*y*+2, −*x*+1, *z*; (iii) −*x*+2, −*y*, −*z*+1; (iv) −*y*+1, *x*−*y*−1, *z*; (v) *y*+1, −*x*+*y*+1, −*z*+1; (vi) −*x*+2, −*y*, *z*+1/2; (vii) *x*, *y*, −*z*+1/2; (viii) −*x*+*y*+1, −*x*+1, *z*; (ix) −*y*+1, *x*−*y*, *z*; (x) −*y*+1, *x*−*y*, −*z*+1/2; (xi) −*x*+*y*+1, −*x*+1, −*z*+1/2. (1)+Y-X,1-X,+Z; (2)+Y-X,+Y,-1/2+Z; (3)+X,1+X-Y,-1/2+Z; (4)1-Y,1+X-Y,+Z; 51-Y,1-X,-1/2+Z; (6)1-Y,1-X,1/2+Z; (7)+Y,+X,1/2-Z; (8)-X,-Y,1-Z; (9)-Y,+X-Y,+Z; (10) -Y+X,-Y,1/2-Z; (11)-Y+X,+X,1-Z; (12)-X,-X+Y,1/2-Z; (13)+Y,-X+Y,1-Z; (14)+Y-X,-X,+Z; (15)+Y,+X,3/2-Z